

COMMUNICATION

Received 00th January 20xx, **Photoreforming of biomass in metal salt hydrate solutions**Christian M. Pichler,^a Taylor Uekert^a and Erwin Reisner^{*,a}

Accepted 00th January 20xx

DOI: 10.1039/x0xx00000x

Metal salt hydrate (MSH) solutions allow for the complete solubilisation of biomass and we demonstrate its use as a reaction medium for the photocatalytic reforming of lignocellulose. Different types of photocatalysts such as TiO₂ and carbon nitride can be employed in MSH to produce H₂ and organic products under more benign conditions than the commonly required extreme pH aqueous solutions.

Photoreforming (PR) allows for the simultaneous production of H₂ gas and organic products from the sunlight-driven conversion of waste polymeric substrates such as biomass and plastics in aqueous medium, ambient temperature and pressure^{1–6} TiO₂ is the archetypical photocatalyst for this process, and CdS quantum dots and carbon nitride (CN_x) have recently been reported as visible-light absorbing alternatives.^{7–11}

Efficient PR requires the substrate to easily access the photocatalyst, which poses a challenge for an insoluble polymeric substrate in combination with a heterogeneous photocatalyst.^{4,12} Lignocellulose is a highly desirable substrate for the PR process due to its abundance as inedible biomass waste and potentially interesting reaction products.¹³ However, its recalcitrance demands harsh reaction conditions such as extremely alkaline or acidic conditions for complete solubilisation.

Employing PR under more benign conditions has the potential to improve the sustainability and efficiency of the process. Lignocellulosic biomass can be solubilised at relatively mild conditions in MSH.^{14–16} Very high concentrations of inorganic salts such as LiBr with low acid concentrations in water can be used to depolymerise lignocellulosic biomass into soluble sugars.^{17–19} Li⁺ coordinates water molecules strongly and

thereby generates acidity that aids cellulose depolymerisation. The presence of Br[−] exhibits favourable hydrogen bonding interactions with the cellulose chain.^{14,19} The majority of studies in MSH have so far solely focussed on the dissolution process of cellulose. Investigations into the chemical conversion of depolymerised cellulose in MSH solutions are rare,^{20,21} and photocatalysis in MSH solutions has not yet been explored.

Here, we report PR of cellulose and real-world lignocellulosic biomass in MSH solutions for the co-production of H₂ gas and soluble organic products (Figure 1). We show the depolymerisation of cellulosic substrates in LiBr MSH solutions, followed by PR of the solubilised sugars with photocatalyst suspension systems based on different TiO₂ and CN_x particles. The influence of LiBr concentration and pH value on PR performance is also investigated.

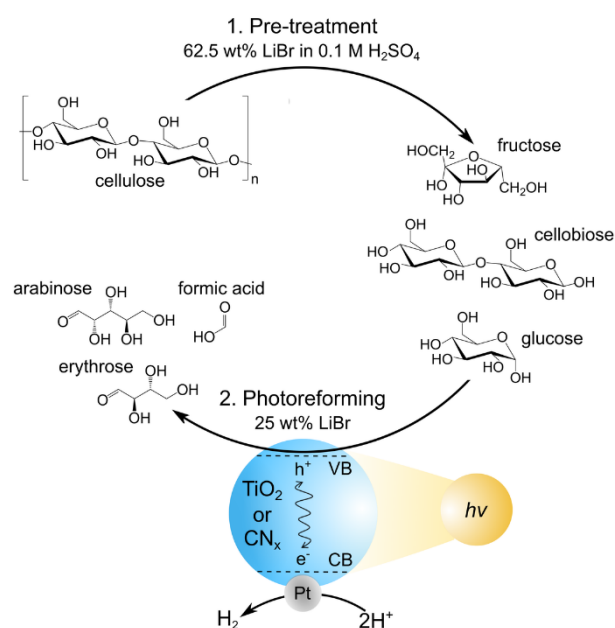


Figure 1. Schematic overview of the PR process in MSH solution.

^a Department of Chemistry, University of Cambridge, Lensfield Road, Cambridge CB2 1EW, United Kingdom, reisner@ch.cam.ac.uk
Website: <http://www-reisner.ch.cam.ac.uk>

† Footnotes relating to the title and/or authors should appear here.
Electronic Supplementary Information (ESI) available: [details of any supplementary information available should be included here]. See DOI: 10.1039/x0xx00000x

First, the dissolution of microcrystalline cellulose (100 mg) in a LiBr MSH solution (2 mL of 62.5 wt% LiBr in aqueous 0.1 M H₂SO₄) at 90 °C open to air was studied. The cellulose was completely dissolved after 30 min and the dissolved products were analysed by high performance liquid chromatography (HPLC) after regular time intervals. Gradual depolymerisation of the cellulose chains into low molecular sugars is observed, with more than 90% of cellulose being converted into glucose, cellobiose and fructose after 5 h (Figure 2). The concentration of cellobiose remains at approximately 20% in the course of the hydrolysis reaction and fructose results from acid-catalysed isomerisation of glucose.

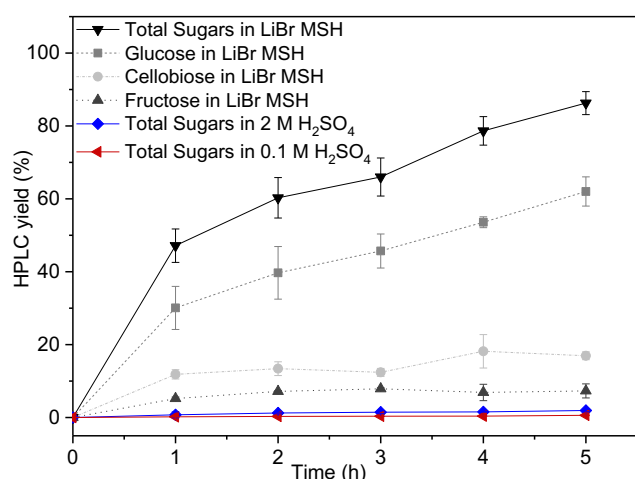


Figure 2. Yield of soluble products from dissolution of microcrystalline cellulose (100 mg) in 2 mL LiBr MSH (62.5 wt% LiBr in 0.1 M H₂SO₄), 0.1 M H₂SO₄ (no LiBr) and 2 M H₂SO₄ (no LiBr) at 90 °C. The yield of total sugars is the sum of glucose, fructose and cellobiose. Bars indicate standard deviation.

For comparison, dissolution of cellulose in aqueous 0.1 M and 2M H₂SO₄ without LiBr was also studied under the same experimental conditions (90 °C). The cellulose remains mostly insoluble in the absence of LiBr-based MSH. Only minor amounts of dissolved sugars are formed by the depolymerisation of the cellulose chains: ~2% total molecular sugars in 2 M H₂SO₄ and <1% in 0.1 M H₂SO₄. The LiBr MSH is therefore crucial for effective cellulose dissolution and depolymerisation.

The cellulose solutions after 5 h MSH treatment were subsequently used for PR with a variety of photocatalyst particles. The photocatalysts were prepared by loading 1 wt% Pt onto different types of TiO₂ (P25, anatase and rutile) nanoparticles and cyanamide-functionalised carbon nitride (N₃CN_x) powder (see ESI for experimental procedures and materials characterisation, Pt particle size 5-15 nm for TiO₂ supports and 3-8 nm for N₃CN_x).^{2,3,22} The latter was employed due to its visible light absorbing properties and high activity to oxidise alcohols, including sugars due to presence of a cyanamide functionality.^{7,8,23-25}

To prepare the standard PR solution, 1 mL of the cellulose lysate in LiBr MSH solution (62.5 wt% LiBr) is added to 1.5 mL H₂O containing 4 mg dispersed photocatalyst (final LiBr concentration: 25 wt%; see Figure 1). This solution is then used for PR during 24 h using simulated solar light irradiation (AM1.5G at 100 mW cm⁻²) with the PR reactor at 25 °C. The amount of H₂ produced from PR is quantified by gas chromatography and the oxidation products by HPLC (dilution of reaction solution 10:1 with H₂O for analysis). PR activities in MSH-free solutions using aqueous H₂SO₄ (2 M) are also shown for comparison. In this case cellulose was pre-treated for 5 h at 90 °C in 2 M H₂SO₄, where only 2% of cellulose are converted into soluble sugars (Figure 2). 1 mL of this solution was diluted with 1.5 mL H₂O and subjected to PR.

The three TiO₂ photocatalysts show a far higher rate of H₂ production in LiBr MSH treated cellulose compared to a control experiment in 2 M H₂SO₄. This result demonstrates the benefit of dissolution and depolymerisation of cellulose in LiBr MSH solution and the compatibility with the PR process. The lower available amount of soluble sugars from the H₂SO₄ treatment results in a lower H₂ yield. The formation rates of oxidation products in Figure 3 for rutile are twice than for P25 and anatase nanoparticles, although the difference in H₂ yield is only around 20%. This difference may be explained by the different reaction mechanisms,²⁶ as rutile forms surface bound radicals and P25/anatase free OH radicals.²⁶ This was confirmed by determining the yield of hydroxy radicals using fluorescence studies in H₂O and 25wt% LiBr solutions (ESI, Figure S3).²⁷

The N₃CN_x photocatalyst shows the lowest activities in both conditions under full spectrum (UV-vis) irradiation. The low performance under acid conditions can be explained by the hydrolysis of cyanamide in N₃CN_x, which also becomes apparent by bleaching of the material over time.^{23,28,29} The hydrolysis of the cyanamide was confirmed by infrared spectroscopy that shows the decline of the characteristic cyanamide peak at 2180 cm⁻¹ under the standard PR conditions (Figure S4).

Despite degradation and lower activity, the N₃CN_x photocatalyst has the benefit of visible light absorption.⁸ PR experiments using cellulose in 25 wt% LiBr with a UV filter ($\lambda > 400$ nm irradiation) produces 49 g_{cat}⁻¹ h⁻¹ H₂ and organic oxidation products with N₃CN_x (Table S1, Entry 16-19 in ESI). The wide-band gap semiconductor TiO₂ did not show any activity with UV-filtered light,³⁰ which is consistent with the previously reported absence of visible light absorbing charge-transfer complexes with TiO₂ and glucose.³¹

To prevent degradation of N₃CN_x, we have also explored basic conditions for PR and added 1 mL cellulose LiBr (62.5 wt%) MSH containing 0.1 M H₂SO₄ into 1.5 mL of aqueous 0.1 M LiOH instead of pure H₂O. The alkaline medium does not significantly hydrolyse the cyanamide-functionality,^{7,8} and enhances the PR performance of the N₃CN_x photocatalyst substantially (giving 112 μ mol H₂ g_{cat}⁻¹ h⁻¹ and also higher yields of organic products). In a control PR experiment with cellulose in 0.1 M

LiOH without LiBr MSH only minor amounts of H₂ (0.8 μmol g⁻¹ h⁻¹) and no organic reaction products were detected (ESI, Table S1, Entry 15). When the alkaline conditions (LiBr MSH + 0.1 M LiOH) are used for the rutile photocatalyst, the H₂ production rate drops from 180 μmol H₂ g_{cat}⁻¹ h⁻¹ (25 wt.% LiBr) to 16 μmol H₂ g_{cat}⁻¹ h⁻¹ (25 wt.% LiBr + 0.1 M LiOH), together with the yield of organic oxidation products (Table S1, Entry 9 in ESI). The decreased photocatalytic activity of TiO₂ in alkaline pH is consistent with previous reports.³²

Next, PR using a real-world lignocellulose substrate was explored. Beech-wood sawdust was treated with LiBr MSH and the wood-lysate is used under standard PR conditions for 96 h using rutile (the best performing TiO₂ photocatalyst for cellulose) and ^{NCN}CN_x during UV-vis irradiation (Figure S5). The MSH depolymerised and dissolved the cellulosic part of wood, while lignin remains undissolved and is filtered off before the start of the PR process. When beech-wood is used the H₂ yield (1.2 μmol H₂ in 24 h for ^{NCN}CN_x) as well as the yield of organic products (0.8 μmol arabinose in 24 h and 1.6 μmol erythrose in 24 h for ^{NCN}CN_x) is lower compared to pure cellulose as substrate, which may be due to the brown colour of the solution from a low concentration of wood degradation products reducing the transmission of light.

Finally, we investigated the role of LiBr in the PR process using glucose as a model substrate.³³ PR of glucose in water was compared with PR under standard conditions (1 mL of the 62.5 wt% LiBr, 0.1 M H₂SO₄ solution is added to 1.5 mL H₂O; final concentration 25 wt% LiBr) using P25, rutile, anatase or ^{NCN}CN_x as catalyst. In pure H₂O, ^{NCN}CN_x is the most active catalyst followed by rutile TiO₂ (ESI, Figure S6). The presence of LiBr under standard conditions changes the relative PR performance substantially: the activity of all three TiO₂ catalysts is reduced by

60-70%, (P25 from 327 to 129, rutile from 436 to 226 and anatase from 322 to 112 μmol H₂ g_{cat}⁻¹ h⁻¹), whereas the H₂ yield for ^{NCN}CN_x is decreased by more than 95% (from 672 to 24 μmol H₂ g_{cat}⁻¹ h⁻¹). Under these conditions, rutile is the most active catalyst. When the MSH concentration is gradually increased from 2.5 to 25% LiBr (including corresponding amounts of H₂SO₄) (ESI, Figure S7) an abrupt decline of activity is observed for ^{NCN}CN_x by losing approximately two thirds of its activity already at 2.5 wt% LiBr (672 to 204 μmol H₂ g_{cat}⁻¹ h⁻¹), whereas the decline for P25 is slower and more gradual (327 μmol H₂ g_{cat}⁻¹ h⁻¹ in pure H₂O and 324 μmol H₂ g_{cat}⁻¹ h⁻¹ at 2.5 wt% LiBr). The reduction in PR activity is consistent with a decrease in adsorption of glucose on the photocatalyst in the presence of LiBr (Figures S6 and S7). It is thus likely that the adsorption of LiBr ions on the heterogeneous catalyst surface blocks adsorption sites for glucose and hinders its photooxidation.³⁴

In conclusion, we demonstrate that MSH solutions are a suitable medium for PR of lignocellulosic biomass. Using MSH offers the advantage that cellulose can be depolymerised under comparably mild conditions to soluble sugars, which can readily access the colloidal photocatalyst during the PR process to produce H₂ as well as arabinose, erythrose and formic acid. Real-world lignocellulosic wood biomass is also shown as suitable substrate for PR in MSH solutions. Our results also show that the presence of high LiBr concentrations reduces the catalytic activity of the photocatalysts, but this deactivation is far outweighed by the drastic enhancement of solubilisation and depolymerisation of polymeric cellulose in biomass PR. We therefore envision that further improvements in biomass PR can be achieved in the future with photocatalysts that do not suffer from partial deactivation from MSH adsorption.

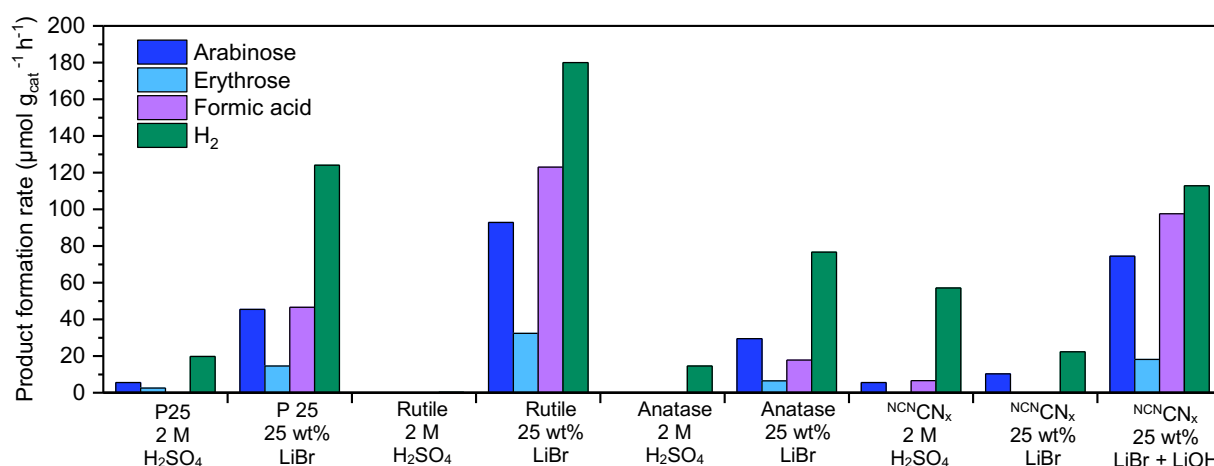


Figure 3. Photoreforming results after 24 h using different photocatalysts and conditions using AM 1.5G, 100 mW cm⁻² irradiation at 25 °C. Cellulose (50 mg) in 1 mL of 62.5 wt% LiBr in 0.1 M H₂SO₄ is added to 1.5 mL aqueous solution containing 4 mg photocatalyst to give 2.5 mL of 25 wt% LiBr. Note that organic products originating from alkaline degradation in the dark were subtracted from the values obtained during PR with ^{NCN}CN_x in 25wt% LiBr with LiOH (see ESI for details). Standard deviations for H₂ yields can be found in Table S1 (between 5-20%). Taking these deviations and the error for the HPLC analysis into account, standard deviation for the organic products can be estimated to be around 20%.

Conflicts of interest

There are no conflicts to declare

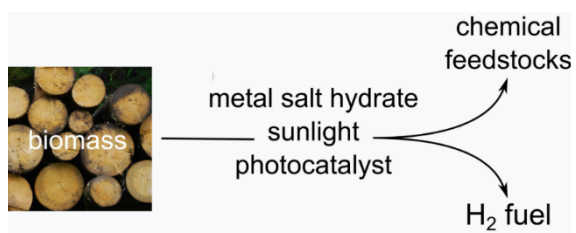
Acknowledgements

Support from the Austrian Science Fund (FWF; Erwin Schrödinger Fellowship J-4381 to C.M.P), EPSRC (nanoDTC, EP/L015978/1 and EP/S022953 to T.U. and E.R.) and OMV (E.R.) is gratefully acknowledged. We also thank Dr Heather Greer for support with electron microscopy and Dr Ana Belenguer for help with HPLC. Dr Tengfei Li and Mr Arjun Vijeta are acknowledged for helpful comments and discussions.

Notes and references

- M. F. Kuehnel and E. Reisner, *Angew. Chemie - Int. Ed.*, 2018, **57**, 3290–3296.
- A. V. Puga, *Coord. Chem. Rev.*, 2016, **315**, 1–66.
- G. Zhang, C. Ni, X. Huang, A. Welgamage, L. A. Lawton, P. K. J. Robertson and J. T. S. Irvine, *Chem. Commun.*, 2016, **52**, 1673–1676.
- T. Uekert, M. F. Kuehnel, D. W. Wakerley and E. Reisner, *Energy Environ. Sci.*, 2018, **11**, 2853–2857.
- T. Kawai and T. Sakata, *Nature*, 1980, **286**, 474–476.
- Q. Xu, Y. Ma, J. Zhang, X. Wang, Z. Feng and C. Li, *J. Catal.*, 2011, **278**, 329–335.
- H. Kasap, D. S. Achilleos, A. Huang and E. Reisner, *J. Am. Chem. Soc.*, 2018, **140**, 11604–11607.
- T. Uekert, H. Kasap and E. Reisner, *J. Am. Chem. Soc.*, 2019, **141**, 15201–15210.
- A. Speltini, M. Sturini, D. Dondi, E. Annovazzi, F. Maraschi, V. Caratto, A. Profumo and A. Buttafava, *Photochem. Photobiol. Sci.*, 2014, **13**, 1410–1419.
- H. Hao, L. Zhang, W. Wang and S. Zeng, *ChemSusChem*, 2018, **11**, 2810–2817.
- D. W. Wakerley, M. F. Kuehnel, K. L. Orchard, K. H. Ly, T. E. Rosser and E. Reisner, *Nat. Energy*, 2017, **2**, 1–9.
- X. Wu, X. Fan, S. Xie, J. Lin, J. Cheng, Q. Zhang, L. Chen and Y. Wang, *Nat. Catal.*, 2018, **1**, 772–780.
- X. Liu, X. Duan, W. Wei, S. Wang and B. J. Ni, *Green Chem.*, 2019, **21**, 4266–4289.
- N. Rodriguez Quiroz, A. M. Norton, H. Nguyen, E. Vasileiadou and D. G. Vlachos, *ACS Catal.*, 2019, **9**, 9923–9952.
- S. Fischer, H. Leipner, K. Thümmel, E. Brendler and J. Peters, *Cellulose*, 2003, **10**, 227–236.
- S. Sen, J. D. Martin and D. S. Argyropoulos, *ACS Sustain. Chem. Eng.*, 2013, **1**, 858–870.
- W. Deng, J. R. Kennedy, G. Tsilomelekis, W. Zheng and V. Nikolakis, *Ind. Eng. Chem. Res.*, 2015, **54**, 5226–5236.
- R. M. de Almeida, J. Li, C. Nederlof, P. O'Connor, M. Makkee and J. A. Moulijn, *ChemSusChem*, 2010, **3**, 325–328.
- N. Rodriguez Quiroz, A. M. D. Padmanathan, S. H. Mushrif and D. G. Vlachos, *ACS Catal.*, 2019, **9**, 10551–10561.
- C. G. Yoo, S. Zhang and X. Pan, *RSC Adv.*, 2017, **7**, 300–308.
- S. Sadula, O. Oesterling, A. Nardone, B. Dinkelacker and B. Saha, *Green Chem.*, 2017, **19**, 3888–3898.
- X. Zhou, Y. Li, Y. Xing, J. Li and X. Jiang, *Dalt. Trans.*, 2019, **48**, 15068–15073.
- V. W. H. Lau, I. Moudrakovski, T. Botari, S. Weinberger, M. B. Mesch, V. Duppel, J. Senker, V. Blum and B. V. Lotsch, *Nat. Commun.*, 2016, **7**, 12165.
- H. Kasap, C. A. Caputo, B. C. M. Martindale, R. Godin, V. W. H. Lau, B. V. Lotsch, J. R. Durrant and E. Reisner, *J. Am. Chem. Soc.*, 2016, **138**, 9183–9192.
- A. Sattler and W. Schnick, *Eur. J. Inorg. Chem.*, 2009, **7**, 4972–4981.
- R. Chong, J. Li, Y. Ma, B. Zhang, H. Han and C. Li, *J. Catal.*, 2014, **314**, 101–108.
- S. Nagarajan, N. C. Skillen, F. Fina, G. Zhang, C. Randorn, L. A. Lawton, J. T. S. Irvine and P. K. J. Robertson, *J. Photochem. Photobiol. A Chem.*, 2017, **334**, 13–19.
- V. W. H. Lau, V. W. Z. Yu, F. Ehrat, T. Botari, I. Moudrakovski, T. Simon, V. Duppel, E. Medina, J. K. Stolarczyk, J. Feldmann, V. Blum and B. V. Lotsch, *Adv. Energy Mater.*, 2017, **7**, 1602251.
- A. Vijeta and E. Reisner, *Chem. Commun.*, 2019, **55**, 14007–14010.
- R. Beranek, *Adv. Phys. Chem.*, 2011, **2011**, 80–83.
- G. Kim, S. Lee and W. Choi, *Applied Catal. B, Environ.*, 2015, **162**, 463–469.
- X. Fu, J. Long, X. Wang, D. Y. C. Leung, Z. Ding, L. Wu, Z. Zhang, Z. Li and X. Fu, *Int. J. Hydrogen Energy*, 2008, **33**, 6484–6491.
- L. Da Vià, C. Recchi, E. O. Gonzalez-Yañez, T. E. Davies and J. A. Lopez-Sanchez, *Appl. Catal. B Environ.*, 2017, **202**, 281–288.
- C. Guillard, E. Puzenat, H. Lachheb, A. Houas and J. M. Herrmann, *Int. J. Photoenergy*, 2005, **7**, 1–9.

Table of Contents artwork



A combined process using LiBr metal salt hydrates and photoreforming converts cellulosic biomass into H₂ and organic reaction products.